Optimization of the Perfectly Matched Layer for the Finite-Element Time-Domain Method

Masoud Movahhedi, *Student Member, IEEE*, Abdolali Abdipour, *Senior Member, IEEE*, Hajdin Ceric, Alireza Sheikholeslami, and Siegfried Selberherr, *Fellow, IEEE*

Abstract—We present a new formulation to implement the complex frequency shifted-perfectly matched layer (CFS–PML) for boundary truncation in 2-D vector finite-element time-domain method directly applied to Maxwell's equations. It is shown that the proposed method is highly absorptive to evanescent modes when computing the wave interaction of elongated structures or sharp corners. The impact of the CFS–PML parameters on the reflection error is investigated and optimal choices of these parameters are derived.

Index Terms—Absorbing boundary conditions (ABC), finite-element time-domain (FETD) method, Maxwell's equations, perfectly matched layer (PML).

I. INTRODUCTION

THE perfectly matched layer (PML) introduced by Bérenger [1] is widely accepted as an efficient numerical absorber used in time-domain electromagnetic solvers. PMLs are often used to implement absorbing boundary conditions (ABCs) in the finite-difference time-domain (FDTD) [1]–[3] and finite-element frequency-domain (FEFD) [4], [5] methods for simulating open-region wave propagation problems. Recently, a PML scheme to truncate finite-element time-domain (FETD) meshes for analyzing 2-D [6] and generally for 3-D [7], [8] open-region electromagnetic scattering and radiation problems has been developed.

Beérenger was first to propose the PML in a split-field formulation for the FDTD method [1]. Different variants were subsequently proposed. Among them, we can state stretched coordinate PML [2], anisotropic-medium (uniaxial) (U)PML [3], [4] and complex-frequency shifted (CFS)-PML [9]. None of these variants require field-splitting and hence have a more appealing physical interpretation. Moreover, they are suitable for finite element applications because they only detail the insertion of new constitutive tensors inside the PML region while keeping the basic form of the Maxwell equations invariant.

To the best of the authors' knowledge, all of the published papers have implemented the PML for the FETD solution of the vector wave equation. In this letter we introduce the PML implementation for the FETD method applied directly to the Maxwell equations. Moreover, instead of using UPML, we use the CFS–PML formulation to improve attenuation of evanescent waves in the simulated structure. The effectiveness of the proposed method is studied as a function of the constitutive parameters of the CFS–PML. Furthermore, the optimized parameters are extracted for FETD method. A numerical example is considered to show the lower reflection errors obtained by our implementation compared to the conventional PML implementation for FETD method.

II. FORMULATION

This section describes the FETD formulation of the CFS–PML for analyzing 2-D open-region radiation electromagnetics problems. Throughout, all fields are assumed to be TE_z polarized; the proposed scheme, however, can also be applied to TM_z problems with minor modifications. Moreover, the method can be easily extended to 3-D problems. Here we consider the PML formulation in the stretched coordinate space [5] for the 2-D TE_z problem. Inside the PML, the fields E and B satisfy the following modified Maxwell's equations in the frequency domain

$$jw\epsilon\tilde{E} = \mu^{-1}\nabla \times \left(\tilde{\bar{\Lambda}}_1(w).\tilde{B}\right) - \tilde{J}$$
$$jw\mu^{-1}\tilde{B} = -\mu^{-1}\nabla \times \left(\tilde{\bar{\Lambda}}_1(w).\tilde{E}\right) \tag{1}$$

where $\tilde{E} = \tilde{E}_x\hat{x} + \tilde{E}_y\hat{y}$ is the electric field and $\tilde{B} = \tilde{B}_z\hat{z}$ is the magnetic flux density in the frequency domain, $\tilde{\bar{\Lambda}}_1(w)$ is a tensor given in Cartesian coordinate by $\tilde{\bar{\Lambda}}_1(w) = (1/\tilde{S}_y(w))\hat{x}\hat{x} + (1/\tilde{S}_x(w))\hat{y}\hat{y}$ and $\tilde{S}_x(w), \tilde{S}_y(w)$ are the stretched-coordinate metrics which are defined as

$$\tilde{S}_i(w) = \kappa_i + \frac{\sigma_i}{\alpha_i + jw\epsilon_0}, \quad i = x, y. \tag{2}$$

In the above equation, σ_i is the conductivity, α_i is assumed to be positive real, and κ_i is real and ≥ 1. We assume that these PML parameters are constant in each element of the FE method. The original form of PML [1] corresponds to $\kappa_i = 1$ and $\alpha_i = 0$, which have been used in [6]–[8]. However, the above CFS form has been shown to have superior properties, particularly for the absorption of evanescent waves.

Transformation of (1) to the time domain using the convention $jw \rightarrow \partial/\partial t$ leads to the equations

$$\epsilon\frac{\partial E}{\partial t} = \mu^{-1}\nabla \times \left(\bar{\Lambda}_1(t) \star B\right) - J$$
$$\mu^{-1}\frac{\partial B}{\partial t} = -\mu^{-1}\nabla \times \left(\bar{\Lambda}_1(t) \star E\right) \tag{3}$$

where $\star$ stands for the convolution. The elements of $\overline{\Lambda}_1(t)$ are given by the Fourier transforms

$$\tilde{S}_i^{-1}(w) \leftrightarrow S_i^{-1}(t) = \frac{\delta(t)}{\kappa_i} - \frac{\sigma_i}{\epsilon\kappa_i^2}e^{-\left(\left(\frac{\sigma_i}{\epsilon_0\kappa_i}\right)+\left(\frac{\alpha_i}{\epsilon_0}\right)\right)t}\overline{u}(t). \quad (4)$$

In (4), $\delta(t)$ is the unit impulse function, and $\overline{u}(t)$ is the unit step function.

In order to obtain the finite element (FE) solution, the examined 2-D domain Ω in the xy-plane is assumed to be discretized by a FE mesh composed by N_t triangular elements and N_e edges. In each point r of the element, Ω^e, the electric field E and the magnetic flux density B are approximated by edge elements and facet elements, respectively, as

$$E^e(r,t) = \sum_{i=1}^{3} e_i(t)W_i(r)$$

$$B^e(r,t) = \sum_{i=1}^{1} b_i(t)F_i(r) \quad (5)$$

where $e_i(t)$ is the electric field circulation along the ith edge, $b_i(t)$ is the flux of the magnetic flux density through ith face, W_i is the Whitney 1-form vector basis function associated to the ith edge, and F_i is the Whitney 2-form vector basis function associated to the ith face [10] such that

$$W \in \mathcal{H}(curl;\Omega) = \left\{u : \nabla \times u \in \left[\mathcal{L}^2(\Omega)\right]^3\right\}$$

$$F \in \mathcal{H}(div;\Omega) = \left\{u : \nabla.u \in \mathcal{L}^2(\Omega)\right\}. \quad (6)$$

To seek the FETD solution of (3) we employ Galerkin's method and use the perfectly electric conducting wall to terminate the PML. By substituting (5) into (3) we obtain the following ordinary differential equations:

$$\sum_{e=1}^{N_t}\left(G_z^e\frac{\partial b}{\partial t} + K^e e + K_x^e\psi_x + K_y^e\psi_y\right) = 0$$

$$\sum_{e=1}^{N_t}\left(C^e\frac{\partial e}{\partial t} - \left(L^e b + L_x^e\varphi_x + L_y^e\varphi_y\right) + q^e\right) = 0 \quad (7)$$

where the matrices are given by

$$G_{z_{ij}}^e = \langle F_i, \mu^{-1}F_j\rangle_{\Omega^e}$$

$$K_{ij}^e = \mu^{-1}\left\langle F_i, \nabla \times \left(\frac{1}{\kappa_y}\widehat{x}.W_j\widehat{x}\right)\right\rangle_{\Omega^e}$$

$$+ \mu^{-1}\left\langle F_i, \nabla \times \left(\frac{1}{\kappa_x}\widehat{y}.W_j\widehat{y}\right)\right\rangle_{\Omega^e}$$

$$K_{x_{ij}}^e = \langle F_i, \mu^{-1}\nabla \times (\widehat{y}.W_j\widehat{y})\rangle_{\Omega^e}$$

$$K_{y_{ij}}^e = \langle F_i, \mu^{-1}\nabla \times (\widehat{x}.W_j\widehat{x})\rangle_{\Omega^e}$$

$$C_{ij}^e = \langle W_i, \epsilon W_j\rangle_{\Omega^e}$$

$$L_{ij}^e = K_{ij}^{e^T}$$

$$L_{x_{ij}}^e = K_{x_{ij}}^{e^T} = \langle F_j, \mu^{-1}\nabla \times (\widehat{y}.W_i\widehat{y})\rangle_{\Omega^e}$$

$$L_{y_{ij}}^e = K_{y_{ij}}^{e^T} = \langle F_j, \mu^{-1}\nabla \times (\widehat{x}.W_i\widehat{x})\rangle_{\Omega^e}$$

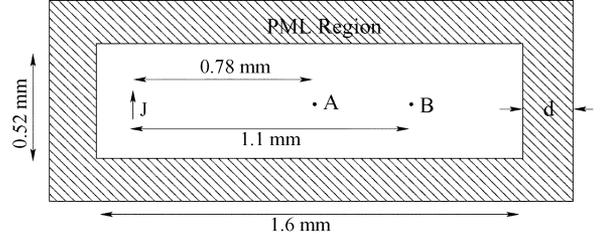$$q_i^e = \langle W_i, J\rangle_{\Omega^e} \quad (8)$$

Fig. 1. Current element J radiating in an elongated FETD grid terminated by CFS–PML.

and ψ_p and φ_p are vectors whose elements can be expressed as

$$\psi_{p,i} = -\frac{\sigma_p}{\epsilon\kappa_p^2}e^{-\left(\left(\frac{\sigma_p}{\epsilon_0\kappa_p}\right)+\left(\frac{\alpha_p}{\epsilon_0}\right)\right)t}\overline{u}(t) \star e_i(t) \quad p=x,y$$

$$\varphi_{p,i} = -\frac{\sigma_p}{\epsilon\kappa_p^2}e^{-\left(\left(\frac{\sigma_p}{\epsilon_0\kappa_p}\right)+\left(\frac{\alpha_p}{\epsilon_0}\right)\right)t}\overline{u}(t) \star b_i(t) \quad p=x,y. \quad (9)$$

In (9), the convolution can be recursively evaluated as [11]

$$\psi_p^n = v_p\psi_p^{n-1} + w_pe^n \quad p=x,y$$

$$\varphi_p^n = v_p\varphi_p^{n-1} + w_pb^n \quad p=x,y$$

$$v_p = e^{-((\sigma_p/\kappa_p+\alpha_p)(\Delta t/\epsilon_0))} \quad p=x,y$$

$$w_p = \frac{\sigma_p}{\sigma_p\kappa_p + \kappa_p^2\alpha_p}\left(e^{-((\sigma_p/\kappa_p+\alpha_p)(\Delta t/\epsilon_0))} - 1.0\right). \quad (10)$$

The global matrices can be obtained from local matrices, and the symbolic summation (7) is carried out easily.

III. NUMERICAL RESULTS

The proposed CFS–PML implementation for the FETD solution of the Maxwell equations is tested on the following example and optimized PML parameters are obtained. This example is designed to measure the reflection from the CFS–PML for approximately tangential incidence. Fig. 1 illustrates the simulated problem involving a current source J radiating TE-polarized waves in an elongated FETD grid. The excitation has the form of a modulated Gaussian pulse. The center frequency and bandwidth of the excitation current are 6×10^{11} Hz and 3.5×10^{11} Hz, respectively. The reflection error in the electric field is computed at point A (0.78 mm from the source) and point B (1.1 mm from the source). A reference solution is obtained by setting the ends sufficiently far. The computational domain is discretized by uniform triangular elements with $\Delta x = \Delta y = 5.2 \times 10^{-2}$ mm. The PML region has a thickness of $d = 3.64 \times 10^{-1}$ mm and is terminated by a perfectly electric wall. The profiles of the PML parameters (σ and κ) are determined by the following:

$$\sigma = \sigma_{\max}\left(\frac{\rho}{d}\right)^m, \quad \sigma_{\max} = -\frac{(m+1)ln(R)}{2\eta d}$$

$$\kappa = 1 + (\kappa_{\max} - 1).\left(\frac{\rho}{d}\right)^m \quad (11)$$

where ρ is the location of an element center, m is the profile order, η is the free space wave impedance, d is the physical depth of the PML region, and R is the theoretical reflection error at normal incidence. α is not scaled and assumed to be constant. As already stated in Section II, the PML parameters are constant in each element and vary from element to element in the PML region.
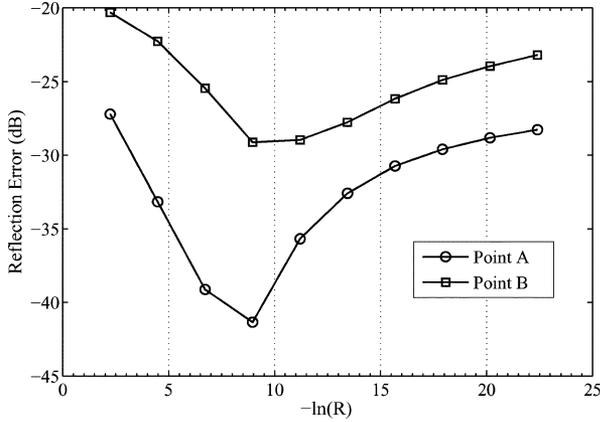
Fig. 2.   Maximum reflection error at points A and B due to a polynomial-scaled CFS–PML versus $-ln(R)$. Parameters $\kappa = 1$, $\alpha = 0$ and $m = 4$.
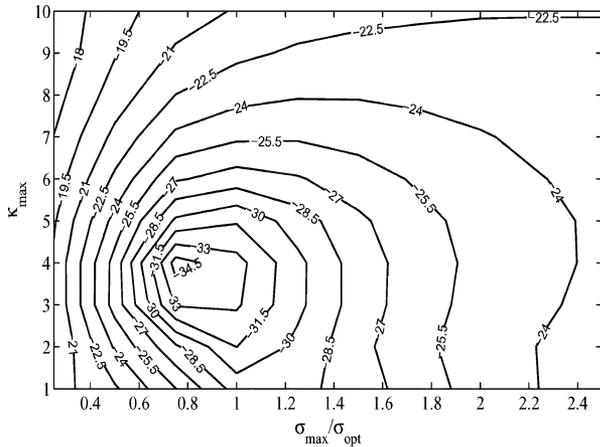

Fig. 3.   Contour plots of the maximum reflection error in dB versus $\kappa_{\max}$ and $\sigma_{\max}/\sigma_{\mathrm{opt}}$ for a polynomial-scaled CFS–PML at point B for $\alpha = 0$.

Fig. 4.   Contour plots of the maximum reflection error in dB versus $\kappa_{\max}$ and $\sigma_{\max}/\sigma_{\mathrm{opt}}$ for a polynomial-scaled CFS–PML at point B for $\alpha = 1.95$.

IV. CONCLUSION

We have described a new CFS–PML implementation for the FETD solution of the Maxwell equations. Moreover, the optimum choices of the CFS–PML parameters have been derived. It was demonstrated that the CFS form of the stretched-coordinate variables enhances its ability to absorb evanescent waves. A maximum reflection error of about -41 dB was recorded for the example, compared to -34 dB for the traditional PML formulation.

The design of an effective PML region requires balancing the theoretical reflection error R and the numerical discretization error. In other words, the optimal values for m, $\sigma_{\max}$, $\kappa_{\max}$ and α should be chosen. We have found that $3 \leq m \leq 4$ to be nearly optimal for this example and some other FETD simulations. To choose the optimal value for $\sigma_{\max}$ we need to determine R. Fig. 2 shows the maximum reflection error recorded at the observation points as a fuction of $-ln(R)$. As it can be seen, an optimal choice for $\sigma_{\max}$, called σ_{opt}, is reached when $R \simeq e^{-9}$. We now note that the radiation due to the current source is characterized by a wide spectrum of waves containing evanescent as well as propagating modes. However, the evanescent modes are not absorbed by the PML when $\kappa = 1$. Increasing κ should help this situation. To investigate this possibility, Fig. 3 plots contours of the maximum reflection error at point B as a function of $\sigma_{\max}/\sigma_{\mathrm{opt}}$ and $\kappa_{\max}$. As expected, this figure shows that increasing $\kappa_{\max}$ leads to a decrease of the reflection error at point B. It is instructive to observe the improvement of the maximum reflection error as a function of α for the complex frequency shifted formulation of PML. Fig. 4 illustrates contour plots of the reflection error versus $\kappa_{\max}$ and $\sigma_{\max}/\sigma_{\mathrm{opt}}$ with $\alpha = 1.95$. It is demonstrated here that the maximum error with $\alpha = 0$ is about -34 dB. With $\alpha = 1.95$, the error is reduced, and is about -41 dB. This is almost a 10 dB improvement over the traditional PML.
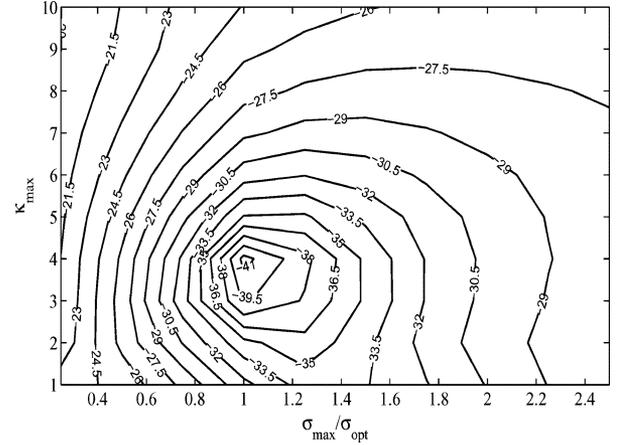
REFERENCES

[1] J. Bérenger, "A perfectly matched layer for the absorption of electromagnetic waves," *J. Comput. Phys.*, vol. 144, no. 2, pp. 185–200, 1994.
[2] W. C. Chew and W. Weedon, "A 3D perfectly matched medium from modified Maxwell's equations with stretched coordinates," *Microw. Opt. Technol. Lett.*, vol. 7, no. 13, pp. 599–604, 1994.
[3] S. D. Gedney, "An anisotropic perfectly matched layer-absorbing medium for the truncation of FDTD lattices," *IEEE Trans. Antennas Propag.*, vol. 44, no. 12, pp. 1630–1639, Dec. 1996.
[4] Z. S. Sacks, D. M. Kingsland, R. Lee, and J. F. Lee, "A perfectly matched anisotropic absorber for use as an absorbing boundary condition," *IEEE Trans. Antennas Propag.*, vol. 43, no. 12, pp. 1460–1463, Dec. 1995.
[5] M. Kuzuoglu and R. Mittra, "Investigation of nonplanar perfectly matched absorbers for finite-element mesh truncation," *IEEE Trans. Antennas Propag.*, vol. 45, no. 3, pp. 474–486, Mar. 1997.
[6] D. Jiao and J.-M. Jin, "An effective algorithm for implementing perfectly matched layers in time-domain finite-element simulation of open-region EM problems," *IEEE Trans. Antennas Propag.*, vol. 50, no. 11, pp. 1615–1623, Nov. 2002.
[7] D. Jiao, J.-M. Jin, E. Michielssen, and D. J. Riley, "Time-domain finite-element simulation of three-dimensional scattering and radiation problems using perfectly matched layers," *IEEE Trans. Antennas Propag.*, vol. 51, no. 2, pp. 296–305, Feb. 2003.
[8] T. Rylander and J.-M. Jin, "Perfectly matched layer in three dimensions for the time-domain finite element method applied to radiation problems," *IEEE Trans. Antennas Propag.*, vol. 53, no. 4, pp. 1489–1499, Apr. 2005.
[9] M. Kuzuoglu and R. Mittra, "Frequency dependence of the constitutive parameters of causal perfectly matched anisotropic absorber," *IEEE Microw. Guided Wave Lett.*, vol. 6, no. 12, pp. 447–449, Dec. 1996.
[10] A. Bossavit, "Whitney forms: a class of finite elements for three-dimensional computations in electromagnetism," *Proc. Inst. Elect. Eng.*, vol. 135, pp. 493–500, 1988.
[11] J. A. Roden and S. D. Gedney, "Convolution PML (CPML): an efficient FDTD implementation of the CFS–PML for arbitrary media," *Microw. Opt. Technol. Lett.*, vol. 27, no. 5, pp. 334–339, 2000.